

Double-resonance spectroscopy of quasi-linear Rydberg states of water

W. L. Glab^{a)}

Department of Physics, Texas Tech University, P.O. Box 41051, Lubbock, Texas 79409

(Received 13 May 2002; accepted 4 September 2002)

We have studied quasi-linear autoionizing Rydberg states of the water molecule with three quanta of bending vibration using double-resonance excitation through the quasi-linear $(\tilde{A})3pb_2$ state. The use of double resonance resulted in vibrational and rotational selectivity which led to simple, easily understood spectra. We have identified and performed an analysis on one ns series and two nd series (σ and π), yielding quantum defects for the series and an improved value of the energy of the ionic state which is the convergence limit for these Rydberg states. At low n , the $4d\pi$ state showed vibronic splitting consistent with the Σ - Δ splitting in the ion core. This splitting vanished at high n as the Rydberg electron uncoupled from the ion core. Comparison of the spectra of bent and linear states in the same energy region displayed the effects of linear-bent interactions on the Rydberg spectrum. © 2002 American Institute of Physics. [DOI: 10.1063/1.1516794]

I. INTRODUCTION

Highly excited states of triatomic molecules are a topic of considerable current interest. Water is a particularly important system for such studies. As a hydride, it possesses relatively large rotational constants, enabling experimenters to more easily resolve complex spectral structures and perform fully quantum state-specific excitation. Considerable progress in understanding the spectrum of Rydberg states converging to the first few vibrational states of the \tilde{X}^2B_1 bent ground state of the ionic core has been made in the last few years, due to the close interaction between new experimental approaches and multichannel quantum defect theory (MQDT). An important advance came with the application of double-resonance techniques to the excitation of these vibrationally autoionizing Rydberg states built on the ground electronic state of the core;¹ as a result of the combining of these new results with an MQDT analysis, the spectrum of these states is now relatively well understood.²

The water ion also possesses a low-lying quasi-linear electronically excited state, the \tilde{A}^2A_1 state, to which series of quasi-linear Rydberg states will converge. The large change in bend angle between the bent ground state of the neutral molecule and the quasi-linear excited state of the ion leads to large Franck-Condon factors only for photoproduction of quasi-linear excited states from the ground state of the neutral which involve a large change in the ν_2 (bending) vibrational quantum number; thus, conventional absorption spectroscopy from the ground state only accesses quasi-linear states with large values of ν_2 . Series of low principal quantum number, high ν_2 states have been observed both using conventional absorption³⁻⁶ and vuv laser absorption spectroscopy.⁷ However, the lowest member of the npb_2 series, the $(\tilde{A})3pb_2$ state, has been excited through two photon absorption, fully resolved, and its spectrum analyzed in detail even for low values of ν_2 .⁸ Photoelectron spectra follow-

ing photoionization of levels of this state seemed to have verified the vibrational numbering from this analysis.⁹ Due to the large change in geometry involved in going from the bent ground state to the $3pb_2$ quasi-linear state, long vibrational progressions in the excited state were observed. Subsequently to this work, however, accurate *ab initio* calculations by Brommer *et al.*¹⁰ indicated that the correct numbering of the bending vibrational states for the linear state of the ion and the linear $(\tilde{A})3pb_2$ state would be to adjust the previously accepted values upwards by 2. We use the revised numbering in this paper.

Quasi-linear Rydberg states of relatively high principal quantum number and low bending vibrational quantum number are expected to overlap the energy region near the first ionization limit of the molecule, which involves leaving the ion in its bent ground state. Such states cannot easily be observed through direct excitation from the bent electronic states of the neutral molecule, due to poor Franck-Condon factors as mentioned above. However, they may serve as important perturbers of the bent Rydberg states lying in the same region of the spectrum through vibronic interactions.¹¹ Indeed, the effects of the presence of this interaction between linear and bent Rydberg states is a remaining question mark in the understanding of the photoabsorption of water near the ionization limit. Selective detection and measurement of the properties of the quasi-linear Rydberg states would go a long way towards resolving this uncertainty.

In this article we present the first observations and analysis of several high n quasi-linear autoionizing Rydberg series of water with three quanta of bending vibrational energy [$(\nu_1=0, \nu_2=3, \nu_3=0)$ or (030) states]. These series show a relatively high state density near the first ionization energy of the molecule, and are thus likely to be significant perturbers of the bent series which have been previously studied and analyzed. These Rydberg states decay both by vibrational and electronic autoionization processes. We have also observed some states of relatively low principal quantum number. Comparison of the spectra of quasi-linear states from

^{a)}Electronic mail: wallace.glab@ttu.edu

TABLE I. Intermediate states used in the experiment, and the Rydberg series excitable from them. The case d ndN^+ states are superpositions of the case b $nd\sigma$ and $nd\pi$ states with the same J .

Intermediate state	Energy (cm ⁻¹)	Rydberg series accessible	
		Case b	Case d
$J'=0$	84 126.6	$ns\sigma$ $J=1$ $nd\sigma$ $J=1$ $nd\pi$ $J=1$	$ns2$ $J=1$ $nd2$ $J=1$ $nd1$ $J=1$
$J'=1$	84 142.6	$ns\sigma$ $J=0,2$ $nd\sigma$ $J=0,2$ $nd\pi$ $J=0,1,2$	$ns1$ $J=0$, $ns3$ $J=2$ $nd1$ $J=0$, $nd3$ $J=2$ $nd0$ $J=0$, $nd1$ $J=1$, $nd2$ $J=2$
$J'=2$	84 174.6	$ns\sigma$ $J=1,3$ $nd\sigma$ $J=1,3$ $nd\pi$ $J=1,2,3$	$ns2$ $J=1$, $ns4$ $J=3$ $nd2$ $J=1$, $nd4$ $J=3$ $nd1$ $J=1$, $nd2$ $J=2$, $nd3$ $J=3$

this experiment with spectra of bent states from previous work² plainly shows the effects of bent-linear electronic perturbations. Selective excitation of the quasi-linear Rydberg states was made possible by the use of double-resonance excitation through selected rotational levels of the (030) vibrational level of the quasi-linear $(\tilde{A})3pb_2$ state.

II. SPECTROSCOPIC BACKGROUND

The vibrational and rotational properties of both asymmetric top molecules (like the bent water states) and symmetric linear triatomic molecules (such as the linear water states) are well known. We restrict ourselves primarily to a discussion of the angular momenta of the states of interest, and how the selection rules determine which Rydberg states will ultimately be excitable with our scheme. The ground state of water has a configuration $(1a_1)^2(2a_1)^2(1b_2)^2(3a_1)^2(1b_1)^2$. Excitation of a $1b_1$ electron leads to several series of bent Rydberg states, the lowest lying and best studied of which is the \tilde{C}^1B_1 state, which has been used as an intermediate state for double-resonance excitation of high n bent states.^{1,2} Promotion of a $3a_1$ electron to the $3pb_2$ orbital leads to a quasi-linear state which has been labeled $(\tilde{A})3pb_2$. In the limit of a linear geometry, the excited electron in this state should be labeled as $3p\sigma_u$, in view of the conservation of the projection of its orbital angular momentum along the linear axis. The electronic symmetry of this state is $^1\Pi_g$. The doubly degenerate bending vibrational modes of this linear configuration lead to the vibrational angular momentum ℓ_v (with possible values of $(0,1,\dots,\nu_2-2,\nu_2)$, which is strongly coupled to the orbital angular momentum to give the vibronic angular momentum projection along the linear axis, K . This state shows rotationally resolved spectra for a number of vibrational states ($0\nu_20$) which have been analyzed by Abramson *et al.*⁸ As mentioned above, it now appears that their vibrational numbering should be revised upwards by 2.¹⁰ In the work of Abramson *et al.* it was demonstrated that the excited states observable in a multiphoton ionization or laser-induced fluorescence experiment all possessed a vibronic quantum number $K=0$; that is, Σ vibronic symmetry. Higher K value states were assumed to be rapidly predissociated. Thus, any levels which are excited from the ground state as the first

step in a double-resonance scheme with intermediate resonance with the $(\tilde{A})3pb_2$ state will have Σ vibronic symmetry.

One-photon excitation from the levels of the $(\tilde{A})3pb_2$ state with low ν_2 values to the region near the ionization limit should result in strong excitation of only quasi-linear Rydberg states, since the vibrational wavefunction overlap with bent states will be poor. Indeed, the excitation will be nearly diagonal in a vibrational sense, with strong excitation of only those quasi-linear Rydberg states with the same value of ν_2 as the intermediate level. Further, since the excitation will occur beginning with a $3p\sigma_u$ electron in a symmetric linear molecule, the angular momentum selection rules will allow the formation of $ns\sigma_g$, $nd\sigma_g$, and $nd\pi_g$ Rydberg orbitals only. This labeling of the Rydberg states is appropriate to the Hund's case b coupling regime, in which the excited electron's angular momentum is still strongly coupled to the molecular frame. We should bear in mind that although the $\Delta\ell = \pm 1$ selection rule is really only a propensity rule in a molecule, in a linear state of a symmetric molecule like water parity will be conserved in the excitation process, so that p orbitals will not be excitable. As higher n values are considered, uncoupling of the orbital angular momentum makes a Hund's case d description of the Rydberg states more appropriate.¹¹ We then view the Rydberg states as being labeled by n , ℓ , the ionic core state quantum numbers ν_1 , ν_2 , ν_3 , the core vibronic angular momentum ℓ_v , the total core angular momentum apart from spin N^+ , and the total angular momentum J . In the experiment we describe here, the $J'=0, 1$, and 2 total angular momentum levels of the (030) vibrational state of the $(\tilde{A})3pb_2$ state were used as intermediate states; thus, we would expect to primarily observe Rydberg states built upon the (030) vibrational state of the linear electronic core state, with total angular momenta determined by the $\Delta J=0, \pm 1$ (but $J=0 \neq J=0$) selection rule. Table I summarizes the series excitable in this experiment.

The only possible values for the vibrational angular momentum of the ion core will be $\ell_v=1$ and 3 for (030) states. We should point out again that we are using the adjusted numbering scheme suggested by Ref. 10 for ν_2 . In the linear ionic \tilde{A} state, the vibrational angular momentum will couple to the excited electrons angular momentum to yield the pos-

sible overall vibronic states. These are labeled with the quantum number for the projection of the total vibronic angular momentum exclusive of spin on the internuclear axis, K , which has possible values of $K = |\Lambda \pm \ell_v|$, where Λ is the projection of the electronic orbital angular momentum on the internuclear axis. For the \tilde{A} state, which has an electronic symmetry of ${}^2\Pi_u$, $\Lambda = 1$. Therefore, the vibronic symmetries which are possible for the ion core in the \tilde{A} state with $\nu_2 = 3$ are Σ and Δ . These states are split by vibronic interactions, and the splittings for a large number of values of ν_2 were measured by Ruett *et al.*¹² using the old, uncorrected numbering scheme. The states we label as (030) would be (010) in the Ruett *et al.* tables; unfortunately, they only list one observed level for what we now consider to be (030). It is possible that the other was missed due to the low intensity of the peaks in their photoelectron spectra for small ν_2 values. The energy of the listed level indicates that it is the Σ state. The Σ – Δ vibronic splitting for (030) should not differ greatly from that of the (050) state, which is calculated to be 42 cm^{-1} from their table.

The addition of a weakly bound Rydberg electron to the linear (030) ionic core will lead to different overall symmetries, depending on the electronic state of the Rydberg electron. In Hund's case *b* where there is significant coupling of the Rydberg electron to the core angular momenta, addition of an $ns\sigma$ or $nd\sigma$ Rydberg electron will lead to Σ and Δ overall vibronic states for the Σ and Δ vibronic states of the core, respectively. The addition of an $nd\pi$ electron will form a state of Π overall vibronic symmetry when combined with a Σ core, and Π and Φ states when combined with a Δ core. In our experiment we will only observe states with Σ and Π overall symmetry since we are exciting from a Σ intermediate state. Thus, for a σ Rydberg electron we will observe only one vibronic state, while for a π Rydberg electron we will observe two states split by the vibronic coupling. One of these transitions, namely the one involving the core in a Δ vibronic state, can occur only because of the presence of vibronic coupling between the Rydberg electron and the core. When the coupling of the Rydberg electron to the core becomes insignificant, at sufficiently high n , the transition to Hund's case *d* is complete. As the vibronic coupling of the Rydberg electron to the core vanishes, the Δ core state transition for $nd\pi$ should have vanishing intensity, and only single peaks converging to levels of the Σ vibronic core state should appear.

The (030) Rydberg states which lie above the lowest ionization energy of water (those with effective quantum number $n^* > 3.3$) but below the energy required to ionize the molecule and leave the ion core in the linear \tilde{A} state will autoionize through an electronic interaction between the quasi-linear Rydberg state and the ionization continua of the bent ground state. The variation of the autoionization rates with principal quantum number will differ from the more familiar case of vibrational autoionization. When a Rydberg state of a polyatomic molecule vibrationally autoionizes, the process generally occurs without any significant change in the geometry of the molecule. Therefore, the Franck–Condon factors which govern the autoionization rate are

nearly diagonal; that is, the process obeys a propensity rule that demands that autoionization occurs with a minimal change in the vibrational state of the ionic core. This means that only a single continuum is important in determining the autoionization rate and the autoionization widths should scale like $1/(n^*)^3$, as the degree of penetration of the core by the Rydberg electron does. Here n^* is the effective principal quantum number. In our case of electronic autoionization, the autoionization rate to a particular final vibrational state will also depend on the Franck–Condon factor between the Rydberg and ionic vibrational states; since the two coupled states have very different geometries, the Franck–Condon factors will be comparable for a significant number of the various possible bent ionic vibrational states. Therefore, it is to be expected that the electronic autoionization rate will decrease more slowly with n^* than in the single continuum case, since new vibrational thresholds are reached as the Rydberg state energy increases. The autoionization widths of the states should consequently scale more slowly with n^* than the penetration of the Rydberg electron into the core region. However, since the Rydberg states may also predisassociate, it will be impossible to draw firm conclusions about the ionization rates from linewidths. An additional expectation is that, due to the selectivity of excitation of (030) linear Rydberg states, the direct photoionization background will be small compared to the resonance peaks; therefore, the observed autoionization lineshapes should be approximately Lorentzian.

Vibrational interactions may also be expected to leave their marks on the spectra; in particular, discrete–discrete perturbations between linear Rydberg states converging to different bending-mode excited linear core states may be quite strong. Such perturbations would reveal their presence through localized energy shifts and linewidth variations, and we see evidence of such perturbations in our spectra as discussed below.

III. EXPERIMENT

High $n\ell$ states converging to the (030) vibrational state of the \tilde{A} quasi-linear state of the ion were excited by stepwise resonant double-resonance excitation from the ground electronic and vibrational state of the neutral water molecule. The excitation process was driven using the light from three pulsed, tunable dye lasers pumped by a single Nd^{+3} :YAG laser (Continuum NY-61) operating at the second and third harmonics at a repetition rate of 10 Hz. The wavelengths required to pump specific rotational lines of the $X(000)$ –(\tilde{A}) $3pb_2$ (030) transition lie in the vacuum ultraviolet (vuv) region of the spectrum, near 118.9 nm. The required vuv light was produced by two-photon resonant difference-frequency generation in krypton gas. A homebuilt tunable dye laser system operating near 606.9 nm was frequency doubled in a KDP crystal; subsequently, the third harmonic of the dye laser light was produced by sum frequency generation in a BBO crystal, yielding several hundred micro-Joules of 202.3 nm light. This light was tuned into two-photon resonance with the $4p^6$ – $4p^55p'$ [$1/2$] $_0$ transition of krypton. The beam from a second laser, tunable around 678

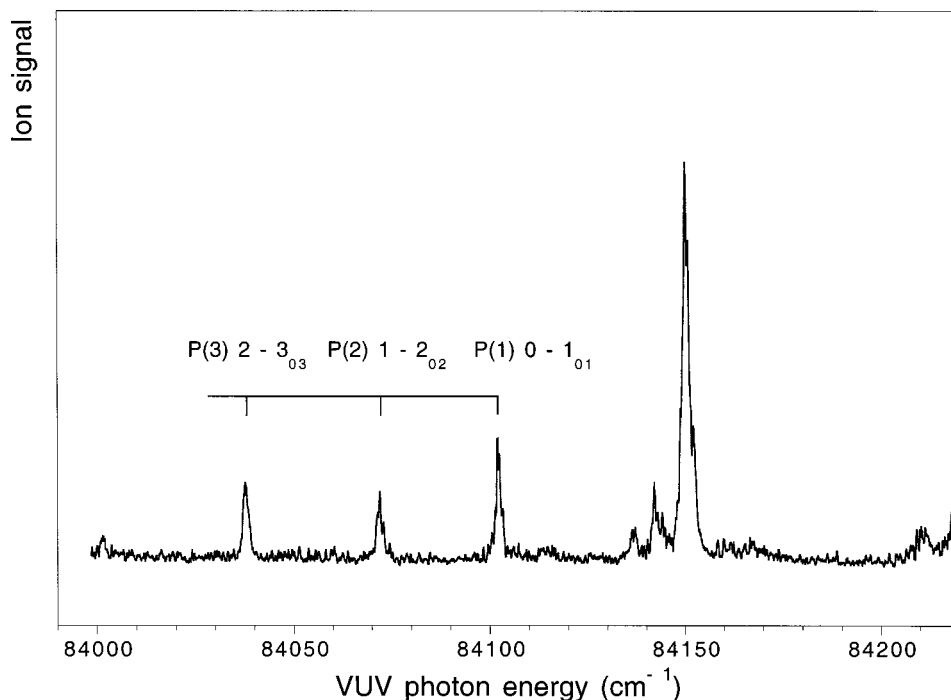


FIG. 1. A portion of the vuv excitation spectrum from the ground state to the $(\tilde{A})3pb_2(030)$ intermediate state with ionization by 355 nm light. The three pump transitions used in this experiment are labeled in the figure.

nm with 2 mJ of pulse energy, was superimposed on the ultraviolet beam using a dichroic mirror. The combined beams were focused using a 15 cm focal length achromatic lens into a cell containing krypton gas at a pressure of about 10 Torr. Vacuum ultraviolet light with photon energy equal to the sum of two of the uv photons minus one of the visible photons exited the cell through a MgF_2 window into the main experimental chamber, which will be described below. No separation of the vuv beam from the fundamental beams was used. We made no attempt to measure the vuv intensity, but previous work suggests that the process should have yielded $\sim 10^{12}$ photons/shot or greater.¹³ The vuv beam diameter in the sensitive volume of our detector was about 2 mm. There was no measurable production of water ions due to the vuv, residual uv, and visible beams. In order to map out the vuv excitation spectrum of the $X(000)-(\tilde{A})3pb_2(030)$ transition, we overlapped the vuv beam with a 10 mJ/pulse beam of 355 nm light from the YAG laser and monitored the one-photon resonant, two-photon ionization which resulted. Figure 1 shows a selected region of the vuv excitation spectrum. In the figure, the first three lines of the P branch, leading to the selective excitation of $J=0, 1,$ and 2 in the excited state are clearly resolved. Rydberg spectra were acquired with the vuv light tuned to each of these lines.

Linear Rydberg states of relatively low principal quantum number ($n < 11$) were excited from the $(\tilde{A})3pb_2(030)$ state using a second homebuilt, tunable dye laser pumped by the third harmonic of the YAG laser. This dye laser operated on a variety of dyes to cover the range of wavelength between 480 and 375 nm. The laser bandwidth was about 0.05 cm^{-1} and pulse energies were about 2 mJ. The beam was counterpropagated with the VUV beam and had a 2 mm diameter. States of higher principal quantum number were excited using a dye laser operating around 750 nm, frequency doubled in BBO using a commercial autotracking

device (Inrad AT-II). The resulting ultraviolet pulse energies were up to $300 \mu\text{J}$. In either case, the dye laser wavelength was scanned under computer control and calibrated using a simultaneously acquired optogalvanic spectrum of neon and uranium lines from a hollow-cathode lamp¹⁴ to an accuracy of roughly 0.1 cm^{-1} .

The experimental chamber consisted of an effusive beam source, a time of flight ion mass spectrometer (TOF-MS), and turbomolecular pumps for evacuation. When no water vapor was flowing into the system, the background pressure was several times 10^{-7} Torr. Water vapor at room temperature and 20 Torr pressure was allowed to flow through a capillary array in the beam source into the main chamber, forming a weakly collimated effusive beam which passed between the plates of the TOF-MS. In operation, the main chamber pressure was about 10^{-5} Torr. The plates had a 1.5 cm separation, and the extraction plate had a nickel-mesh covered 3 mm diameter hole through which ions passed into the flight tube. Ions were extracted with a 200 V/cm field pulse which was delayed with respect to the lasers by 50 ns, so that the laser excitation/ionization process occurred under field-free conditions. The ions were mass analyzed in the 50 cm long flight tube flight before detection with a channeltron, thereby separating the water ions due to Rydberg state autoionization from background ions due to photodissociation and ionization of organic impurities in the vacuum. Up to several thousand ions/laser shot were detected on strong transitions.

IV. OBSERVED RYDBERG SPECTRA AND ANALYSIS

A. High principal quantum numbers: $n \sim 8$ and up

Figure 2 shows the observed spectrum of quasi-linear (030) Rydberg states for $n = 11$ and above, excited from the

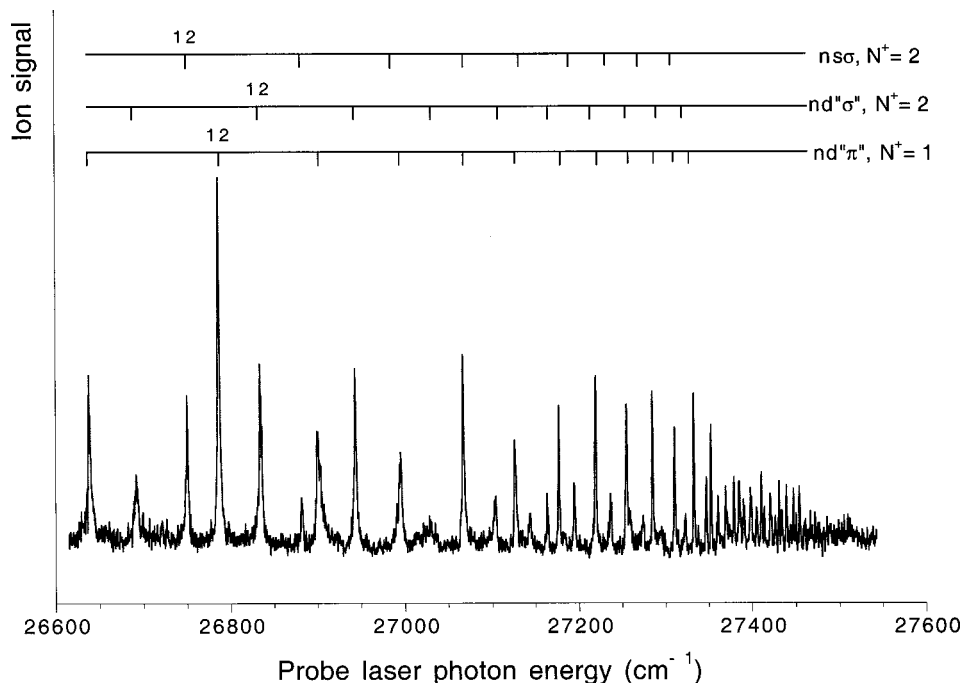


FIG. 2. The spectrum of $R(0)$ transitions to $J=1$ final Rydberg states with (030) vibrational state in the region of energy covering $n=12$ and above, vs probe laser photon energy. The identifications of the series responsible for the peaks are included with the rotational state of the core to which each series converges. All of the observed peaks are due to states with three quanta of bending vibrational energy. The intermediate state energy for this spectrum is $84\,126.6\text{ cm}^{-1}$ (from Ref. 8).

$J'=0$ rotational level of the linear $(\tilde{A})3pb_2$ (030) state. The $J'=0$ level was excited from the 1_{01} level of the neutral ground state in a $P(1)$ transition; since this initial state is the para modification, the Rydberg states will also be para. Higher J states of the intermediate state are of mixed ortho-para character. For this spectrum, the Rydberg states were excited from the intermediate state using the frequency-doubled dye laser. The selection rule for total angular momentum J dictates that all transitions seen in this spectrum are $R(0)$ transitions to $J=1$ final Rydberg states, while the accessible Rydberg orbitals will be $ns\sigma$, $nd\sigma$, and $nd\pi$. Well-resolved peaks are seen from $n=11$ up to $n\sim 30$. For principal quantum numbers this high, Hund's case d should be the appropriate description for the angular momentum coupling of the Rydberg electron to the ion core; consequently, the observed series should be assignable as converging to specific rotational states of the ion core, N^+ . The peaks seen here belong to two distinct series which converge to $N^+=2$ of the (030) Σ vibronic state of the ion, and one which converges to $N^+=1$, of the same core vibronic state based on fits to the observed energies to a simple Rydberg formula including a constant quantum defect,

$$\epsilon_{n,\ell,N^+} = \text{IP}(N^+) - \frac{(\text{Ry})_{\text{water}}}{(n - \delta_{\ell,N^+})^2},$$

where $\text{IP}(N^+)$ is the energy of the convergence limit of the series in question, $(\text{Ry})_{\text{water}}$ is the Rydberg constant for water, $109\,732\text{ cm}^{-1}$, and δ_{ℓ,N^+} is the quantum defect of the series. The experimentally determined Rydberg state energies for the $J=1$ states are given in Table II. The fitted results for the series, which are identified as $ns\sigma$ and $nd''\sigma''$ (converging to $N^+=2$) and $nd''\pi''$ (converging to $N^+=1$), are listed in Table III, along with the statistical errors associated with the fits (the parentheses in the state labeling reflects the fact that the projection λ is not a good quantum number for these

high n states). The identifications of the series are based on the quantum defects and the analysis of the spectra from higher J levels of the intermediate state, to be presented below. The Hund's case d identifications for the observed $J=1$ Rydberg states are also given in Table II, along with the difference in energy between the experimental values and the values calculated from the Rydberg fits (residuals). The s Rydberg states would be expected to have a rather large quantum defect, while the d states would have quantum defects of ~ 0.1 or smaller as the results show. The $nd''\pi''$ series ($nd1$ in Hund's case d), due to its relatively high intensity and the large number of peaks identified, results in an accurate determination of the energy of the (030) Σ $N^+=1$ ionization limit relative to the ground state of the neutral molecule, $111\,688.3 \pm 0.5\text{ cm}^{-1}$. Since the rotational energies for a linear state are given by $B^+N^+(N^++1)$, this number can be adjusted downwards by $2B^+$ (where $B^+ \sim 8.9\text{ cm}^{-1}$ is the rotational constant of the ion in the linear state, as given below) to give the (030) $N^+=0$ ionization limit as $111\,670.5 \pm 1.0\text{ cm}^{-1}$. This is in agreement with the photoelectron spectroscopy result of Ruett *et al.*¹² of $111\,641 \pm 30\text{ cm}^{-1}$, but of course much more accurate. The energy separation of the two fitted series limits yields a value of the rotational constant of the $(\tilde{A})3pb_2$ (030) state of $8.9 \pm 0.4\text{ cm}^{-1}$, in good agreement with previous results.¹⁵ We have been unable to identify any transitions to Rydberg states with a Δ ionic core state in this spectrum, indicating that the uncoupling of the Rydberg angular momentum from that of the core (transition to Hund's case d) is essentially complete by $n\sim 11$.

One frequently sees strong interactions between Rydberg series which converge to different ionic rotational states in molecular Rydberg spectra. These rotational interactions can lead to large energy shifts and intensity variations in localized regions of the spectra where there is near-degeneracy

TABLE II. Observed $J=1$ Rydberg state energies and identifications. Energies are total energy above the ground state of the neutral molecule in cm^{-1} , including the $J'=0$ intermediate state energy of $84\,126.6\text{ cm}^{-1}$. The Rydberg state identifications are given in Hund's case d notation, $n\ell N^+$. When comments indicate that blending of two lines, the comments are given with the state which would be expected to be more intense based on neighboring transitions. The n labeling is appropriate for quantum defects with magnitude less than unity. The number in parentheses following each entry is the difference between the experimental value and the value calculated from the fit parameters in Table III, in cm^{-1} .

n	$nd1$	$nd2$	$ns2$	Comments
11	110 765.2 (0.7)			
11		110 818.6 (3.0)		
12			110 876.8 (-2.0)	
12	110 913.2 (-0.1)			
12		110 960.8 (0.5)		
13			111 008.4 (-1.9)	
13	111 027.3 (-1.5)			broad, shaded to blue
13		111 070.0 (-2.9)		
14	111 121.8 (1.5)			blend with 14s2, shaded to red
15	111 193.5 (-0.5)			blend with 15s2
15		111 230.6 (-3.7)		
16	111 253.0 (-1.3)			
16			111 270.3 (7.7)	
16		111 290.0 (-3.3)		
17	111 303.8 (-0.3)			
17			111 321.1 (3.6)	
18	111 346.0 (0.1)			blend with 17d2
18			111 363.0 (-0.3)	
19	111 381.7 (0.5)			blend with 18d2
19			111 400.5 (-1.2)	
20	111 411.5 (0.2)			
21	111 437.2 (0.1)			
20		111 449.4 (2.0)		
22	111 459.6 (0.0)			blend with 21s2
21		111 473.8 (0.9)		
23	111 479.0 (-0.1)			
22			111 487.1 (0.6)	
24	111 496.0 (-0.3)			blend with 22d2
23			111 505.5 (-2.0)	
25	111 511.5 (0.1)			blend with 23d2
23		111 517.0 (2.7)		
26	111 524.8 (0.0)			blend with 24s2
24		111 531.7 (0.5)		
27	111 537.0 (0.3)			
25			111 540.3 (-1.7)	
28	111 547.2 (-0.2)			
26			111 553.4 (-2.9)	
29	111 557.3 (0.3)			
26		111 560.4 (1.1)		
30	111 565.6 (0.0)			blend with 27s2
27		111 570.2 (-0.9)		
31	111 573.7 (0.2)			

between Rydberg states with differing values of n and N^+ . The natural theoretical framework for the interpretation of such series interactions is multichannel quantum defect theory (MQDT). Close examination of the residuals in Table II, in particular for the $nd''\pi''$ ($nd1$) series, shows that the localized energy perturbations expected from a rotational series interaction are in fact too small to be discerned; that is, the residuals are generally not much greater than the accuracy with which the line positions can be measured. The only apparent actual perturbation observable in this series is believed to be vibrational in nature, and is discussed below. We conclude that a MQDT analysis of rotational interactions is unnecessary for the interpretation of the spectra of the high n

$J=1$ states. A full MQDT treatment including both rotational and vibrational interactions will become possible when further spectroscopic data is available.

The linewidths of the observed transitions are considerably greater than our experimental resolution over the whole range presented, and are not significantly different for the different electronic states. Simple arguments based on the degree of core penetration of the Rydberg orbitals would suggest that the s states should be significantly broader than the d states. The fact that this is not observed may be due to strong $s-d$ mixing by the nonspherically symmetric ion core, which has already been noted in the Rydberg states of molecular hydrogen.¹⁶ There is a trend towards smaller line-

TABLE III. Results of fits to a Rydberg formula with constant quantum defects for the $J=1$ series. Energies are given in wave numbers, and the uncertainty in the last digit is given in parentheses. The series limit energies include the energy of the $(\bar{A})3pb_2(010)J'=0$ intermediate state above the ground state of the neutral molecule, $84\,126.6\text{ cm}^{-1}$.

Series	Limit	Quantum defect
$nsN^+=2$	111 726 (2)	0.624 (5)
$nd''\sigma''N^+=2$	111 722 (2)	-0.010 (5)
$nd''\pi''N^+=1$	111 688.3 (5)	0.102 (3)

widths with increasing principal quantum number, as would be expected from simple scaling arguments based on the probability of the Rydberg electron colliding with the ion core. Near $n=12$, linewidths are typically $3\text{--}5\text{ cm}^{-1}$, near $n=15$ they are $2\text{--}3\text{ cm}^{-1}$, and near $n=20$ they are about $2.5\text{--}2\text{ cm}^{-1}$. Even in view of a $\sim 1\text{ cm}^{-1}$ contribution to the linewidths from the lifetime broadening of the intermediate state levels, this is a less pronounced variation than the n^{*-3} dependence which would govern the widths if autoionization was to a single continuum, indicating that the decrease in autoionization rates due to reduced core penetration as n increases is moderated by the opening of new ionization channels as bent vibrational thresholds are passed. Predissociation undoubtedly contributes to the overall linewidths as well, due to Renner–Teller coupling of the linear states to the bent A_2 states as discussed by Dixon.¹⁷

There is a rather pronounced deviation from the smooth trend of linewidth decrease with n for the $nd\pi$ series at $n=13$ and 14 , where the linewidths of these peaks are considerably larger than the neighboring peaks, as shown in Fig. 3. Additionally, these two peaks show asymmetric profiles, with $n=13$ shaded to the blue and $n=14$ shaded to the red. Figure 3 also shows the deviations of the measured transition energies for the $nd\pi$ series from the Rydberg fit results, and shows a dispersionlike deviation for these two peaks. These

features strongly suggest that a perturbing state lies between the $n=13$ and $n=14$ states. The perturbing state must have the same symmetry as the Rydberg states and the same value of J , as demanded by the perturbation selection rules. Additionally, the perturber and the Rydberg states must have significant overlaps of their vibrational wave functions to yield a strong perturbation. The most likely possibility is that of a vibrational interaction with the $(050)7d\pi N^+=1$ state, whose calculated energy [based on the (030) quantum defect and the ionic vibrational energy differences of Ruett *et al.*¹¹] of $111\,060\text{ cm}^{-1}$ falls in between the $n=13$ and $n=14$ $nd''\pi''$ states.

Figure 4 shows a part of the spectrum of Rydberg state transitions in excitation from the $J'=1$ rotational level of the intermediate state, while Fig. 5 shows the same part of the spectrum for excitation from the $J'=2$ rotational level. For these situations, P , Q , and R branch transitions terminating in $J=0, 1$, and 2 Rydberg states are possible. The principal quantum numbers in these spectra are lower than in the previous spectrum, so that a Hund's case b labeling might be more appropriate in this case than Hund's case d labeling. Since the intermediate state is a state of overall Σ symmetry, transitions to final $nl\sigma$ states will show only P and Q branches, and transitions to $nd\pi$ states should have intense Q branches and weak P and R branches. This is observed in the spectra. The most intense series is $Q(1)nd\pi$, while the corresponding P and R branch transitions are too weak to be clearly identified in the spectra. The P and R branch transitions to $ns\sigma$ are also fairly intense, while transitions to $nd\sigma$ are weak. Each of these spectra show the $Q(J)9d\pi$ transitions to be significantly broadened. This is most likely due to perturbation by the $(050)6d\pi$ states which are nearly degenerate in energy with the upper states of these broadened transitions. As in the spectrum of $J=1$ Rydberg states, no vibronically induced transitions to states with a Δ core vibronic state are observed.

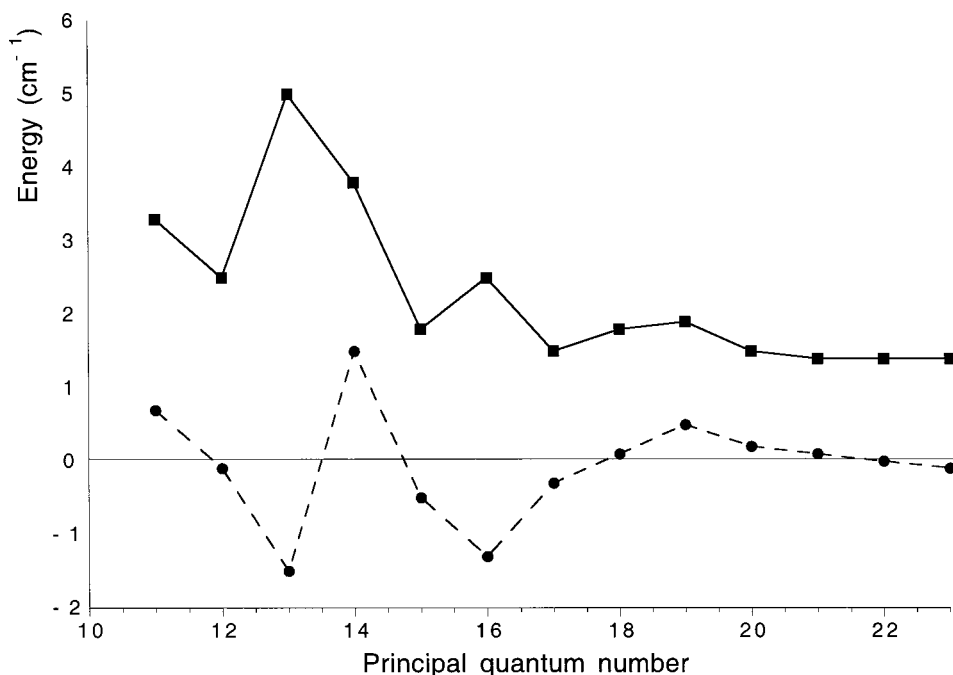


FIG. 3. The solid dots in this figure give the residuals between the Rydberg fit and the observed energies for the $J=1$ $nd\pi$ series as a function of principal quantum number, while the squares give the full width at half-maximum of the corresponding peaks. The peak widths and residuals are large near $n=13\text{--}14$, betraying the presence of a perturbing state.

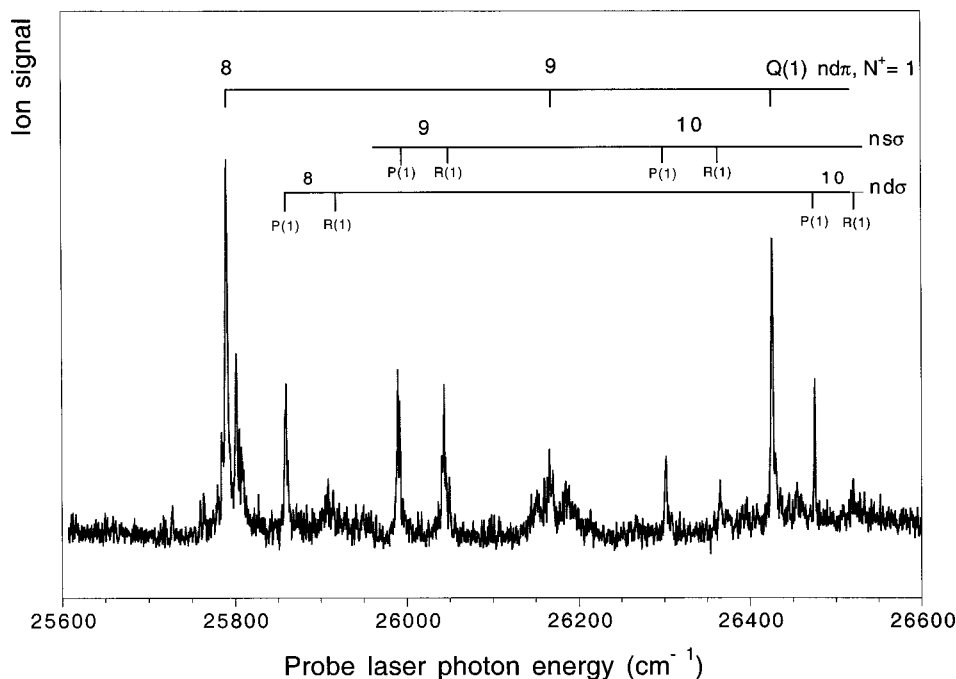


FIG. 4. Spectrum of $P(1)$, $Q(1)$, and $R(1)$ transitions from the $J'=1$ intermediate state, vs probe laser photon energy. The intermediate state energy is $84\,143.6\text{ cm}^{-1}$. The $nd\pi$ series shows a strong Q branch and nearly absent P and R branches, as expected for a transition from a Σ to a Π vibronic state. The $ns\sigma$ and $nd\sigma$ series show P and R branches only, as expected for Σ - Σ transitions. The relatively low intensity and large width of the $9d\pi$ transition is believed to be due to a vibrational perturbation, as discussed in the text. Some of the substructure in the lower $n\pi$ states may be due to small vibronic splittings.

B. Low n transitions and linear-bent interactions

We have also acquired spectra of some transitions to linear Rydberg states of relatively low principal quantum number. It is these states that lie in the vicinity of the first ionization limit, and would therefore be expected to cause perturbations in the spectra of bent Rydberg states.

Figure 6 shows the $P(1)$ and $R(1)$ transitions to the $5s\sigma$ state. The peaks have a width of about 9 cm^{-1} and are separated by 49.0 cm^{-1} , implying a rotational constant of 8.2 cm^{-1} for this state. This is a reasonable value, between the ionic ($\sim 9.0\text{ cm}^{-1}$)¹⁴ and $(\tilde{A})3pb_2(030)$ state⁸ (8.0 cm^{-1}) values, indicating an intermediate value for the bond length in the $5s$ state. The spectrum of the $P(2)$ and $R(2)$ transi-

tions show similar widths and an energy spacing consistent with the rotational constant given above. The fact that the widths depend weakly, if at all, on the rotational quantum number indicates that the principal decay mechanism for this state is governed by a homogeneous coupling.

Figure 7 shows the spectrum of $J=1$ Rydberg states in the energy region of $n=4$, acquired in excitation from the $J'=0$ intermediate state. There are two groups of two transitions each, the lower energy of which is assigned to $4d\pi$ and the other to $4d\sigma$ based on their quantum defects. The $4d\pi$ peaks are roughly equal in intensity and have similar widths of $\sim 15\text{ cm}^{-1}$. The splittings within the $4d\pi$ electronic state are due to vibronic interactions, as discussed

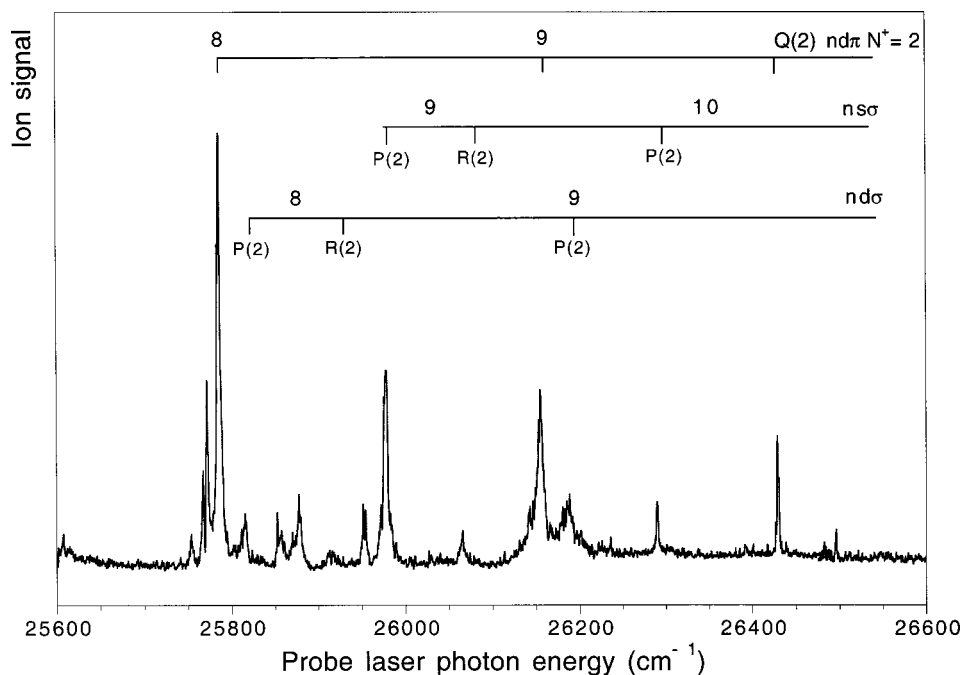


FIG. 5. Spectrum of $P(2)$, $Q(2)$, and $R(2)$ transitions from the intermediate state, vs probe laser photon energy. The intermediate $J'=2$ state energy is $84\,175.6\text{ cm}^{-1}$. As in the previous spectrum, the most intense series is the Q branch of the $nd\pi$ series. As in the previous spectrum, the relatively low intensity and large width of the $9d\pi$ transition is believed to be due to a vibrational perturbation.

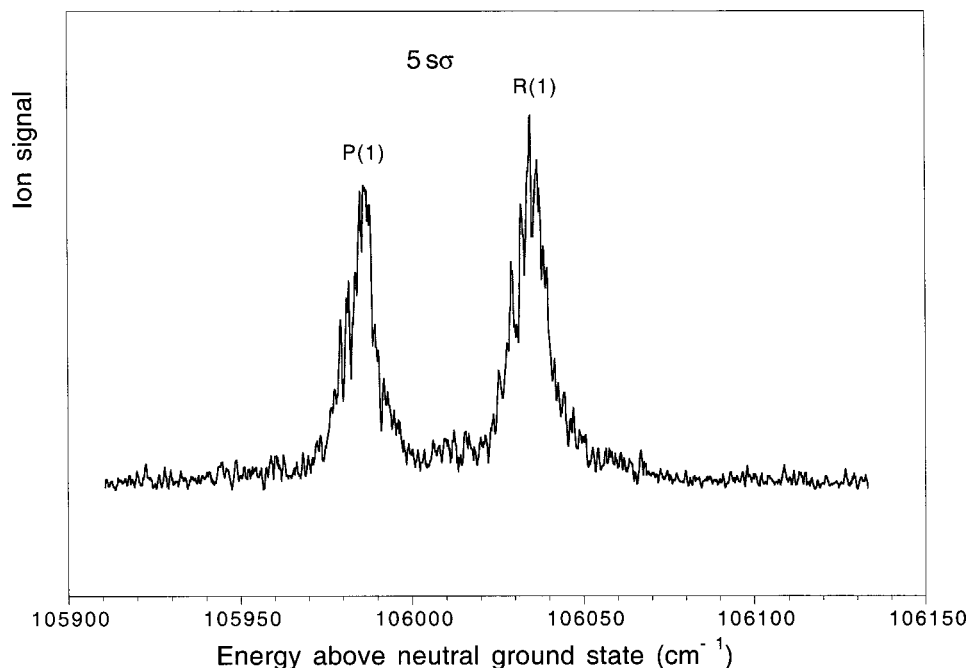


FIG. 6. $P(1)$ and $R(1)$ transitions to the $5s\sigma$ state. The peak separation implies a rotational constant of 8.2 cm^{-1} . The widths are nearly independent of the angular momentum quantum number, indicating a homogenous mechanism for the decay of the excited state.

above. The separation between the subcomponents of the $4d\pi$ state is 42 cm^{-1} , while the subcomponents of the $4d\sigma$ state are separated by 16 cm^{-1} . The splitting of the $4d\pi$ peak, which results from the coupling of the two possible Π overall vibronic states, is the same as the expected vibronic splitting of the Σ and Δ core vibronic states. This indicates that the vibronic coupling of the Rydberg electron to the core is sufficient to vibronically induce the transition to the Rydberg state with a Δ core, but not large enough to significantly alter the Renner–Teller coupling and the splitting.

The splitting of the $4d\sigma$ peak is harder to rationalize. As discussed above, only a single vibronic state should be accessible for a σ Rydberg electron. A further piece of infor-

mation is the fact that the lower energy component of the peak is much narrower than the higher energy component. It is likely that the narrowness of the lower energy peak indicates that it appears in the spectrum due to a mutual perturbation between the $4d\sigma$ state and a bent Rydberg state converging to a vibrationally excited limit. The mixing between these states would lead to intensity borrowing by the bent perturber. It is impossible at this time, based on the available spectroscopic information, to identify the bent perturber.

Figure 8 is a comparison between the spectrum of autoionizing bent (100) $J=1$ Rydberg states excited from the $\tilde{C}(100)$ intermediate state with the spectrum of the $4d\pi$

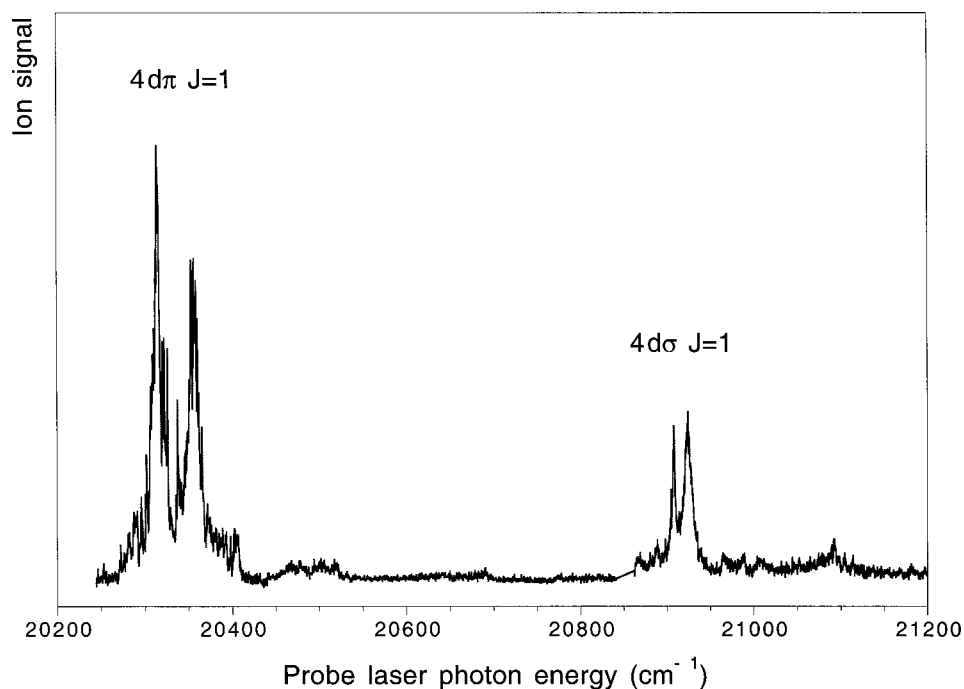


FIG. 7. Spectrum of the $R(0)$ transitions to $4d\sigma$ and $4d\pi$ (030) states. The splittings of these peaks are discussed in the text.

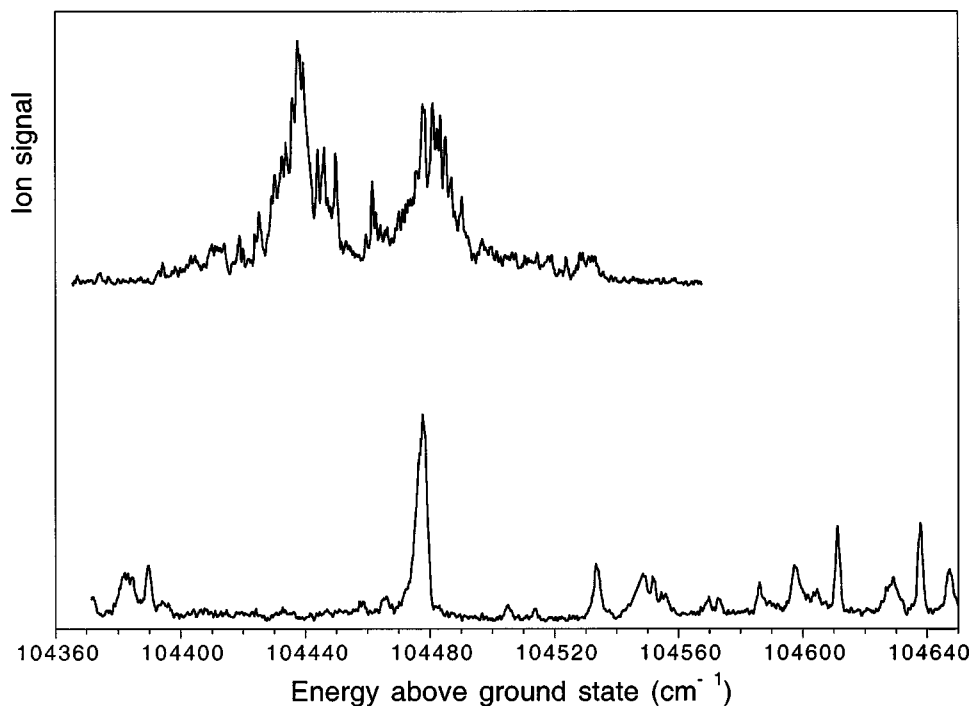


FIG. 8. A comparison of the spectrum of $J=1$ Rydberg states excited from the quasi-linear $(\tilde{A})3pb_2$ (030) intermediate state and the bent $\tilde{C}(100)$ state, showing the effects of linear-bent interactions as discussed in the text. The top trace shows the quasi-linear $4d\pi$ transitions, while the bottom trace is the excitation spectrum of bent Rydberg states converging to the (100) vibrational level of the ground electronic state of the ion.

(030) $J=1$ quasi-linear state excited from the $(\tilde{A})3pb_2$ (030) state in an energy region ~ 2800 cm^{-1} above the ionization energy of the molecule. The (100) bent Rydberg state spectrum in this energy region has been analyzed with MQDT.² It is a region in which the intensities of the bent Rydberg state transitions are disturbed by a perturbation, the nature of which was not determined by the analysis. This figure shows that the region of disturbed intensities coincides in energy with the location of the linear $4d\pi$ $J=1$ states, suggesting that this is an example of linear-bent perturbation. In particular, intensities of transitions to bent Rydberg states from the $\tilde{C}(100)$ state are strongly suppressed in the vicinity of the $4d\pi$ states, with the exception of a strong transition at 104477 cm^{-1} which lies between the two components of $4d\pi$. This lowering of the apparent intensity of these transitions might be explained in terms of the decay dynamics of the Rydberg states as follows. If the $4d\pi$ state decays predominantly by predissociation, the presence of mixing with this state might induce a dissociation rate large enough to overwhelm the relatively low autoionization rate of the high n bent Rydberg states, with the result that they vanish from the ionization spectrum in this energy region. The presence of the single strong peak in this region excited from the $\tilde{C}(100)$ state might then be explained as an interference cancellation of the predissociation probability amplitudes induced through mixing with the two vibronic components of the $4d\pi$ state.

V. CONCLUSION

Double-resonance excitation using combined vuv and visible/near uv laser light and intermediate resonance with a quasi-linear intermediate state has made it possible for us to study quasi-linear Rydberg states of water in some detail. The use of fully quantum state specific excitation in the first

step of the double-resonance process leads to Rydberg spectra on the second step which are relatively simple, since the Rydberg states are excited essentially without a change in vibrational state, and the final state angular momenta are determined by selection rules. Our observations have allowed us to identify a number of series of high principal quantum number states converging to several rotational levels of the linear \tilde{A} state of the ion core, as well as determining the energies of the series limits and the series quantum defects by fitting the observed state energies to a simple Rydberg formula. We have also observed some lower principal quantum number states; in particular, spectra of the $4d\pi$ state show vibronic splitting due to the Renner–Teller effect. Comparison between the spectrum of quasi-linear states excited from the linear intermediate state and a spectrum in the same energy region excited from the bent \tilde{C} state explicitly shows effects of electronic coupling between linear and bent states. Future work which will examine both quasi-linear and bent Rydberg states with higher vibrational excitation is planned, to build up a broader picture of the effects of bent-linear interactions which will provide the experimental basis for a more comprehensive multichannel quantum defect theory of the Rydberg states of water.

ACKNOWLEDGMENTS

This work was supported by the Robert A. Welch Foundation under Grant No. D-1204. The author would like to thank Professor M. S. Child for a critical reading of the manuscript and helpful suggestions, The assistance of Brent Caldwell is also gratefully acknowledged.

¹W. L. Glab, J. Chem. Phys. **107**, 5979 (1997).

²M. S. Child and W. L. Glab, J. Chem. Phys. **112**, 3754 (2000).

³D. H. Ktatyama, R. E. Huffman, and C. L. O'Bryan, J. Chem. Phys. **59**, 4309 (1973).

- ⁴P. Gürtler, V. Saile, and E. E. Koch, *Chem. Phys. Lett.* **51**, 386 (1977).
- ⁵E. Ishiguro, M. Sasanuma, H. Matsuko, Y. Morioka, and M. Nakamura, *J. Phys. B* **11**, 993 (1978).
- ⁶P. M. Dehmer and D. M. P. Holland, *J. Chem. Phys.* **94**, 3302 (1991).
- ⁷R. H. Page, R. J. Larkin, Y. R. Shen, and Y. T. Lee, *J. Chem. Phys.* **88**, 2249 (1988).
- ⁸E. H. Abramson, J. Zhang, and D. G. Imre, *J. Chem. Phys.* **93**, 947 (1990).
- ⁹S. T. Pratt, J. L. Dehmer, and P. M. Dehmer, *Chem. Phys. Lett.* **196**, 469 (1992).
- ¹⁰M. Brommer, B. Weis, B. Follmeg, P. Rosmus, S. Carter, N. C. Handy, H.-J. Werner, and P. J. Knowles, *J. Chem. Phys.* **98**, 5222 (1993).
- ¹¹M. S. Child and C. Jungen, *J. Chem. Phys.* **93**, 7756 (1990).
- ¹²J. E. Ruett, L. S. Wang, Y. T. Lee, and D. A. Shirley, *J. Chem. Phys.* **85**, 6928 (1986).
- ¹³G. Hilber, A. Lago, and R. Wallenstein, *J. Opt. Soc. Am. B* **4**, 1753 (1987).
- ¹⁴B. A. Palmer, R. Engleman, Jr., and E. F. Zalewski, "An Atlas of Uranium Emission Intensities in a Hollow Cathode Discharge," Los Alamos Scientific Laboratory Report No. LA-8251-MS (unpublished).
- ¹⁵H. Lew, *Can. J. Phys.* **54**, 2028 (1976).
- ¹⁶S. C. Ross and C. Jungen, *Phys. Rev. A* **49**, 4353 (1994).
- ¹⁷R. N. Dixon, *Mol. Phys.* **54**, 333 (1985).